

## Complex exposure history of pre-LGM glacial drifts in Terra Nova Bay, Victoria Land, using a multiple cosmogenic nuclide approach

L. Di Nicola,<sup>1,3</sup> S. Strasky,<sup>2</sup> C. Schlüchter,<sup>3</sup> M. C. Salvatore,<sup>4</sup> P. W. Kubik,<sup>5</sup> S. Ivy-Ochs,<sup>6</sup> R. Wieler,<sup>2</sup> N. Akçar,<sup>3</sup> and C. Baroni<sup>7</sup>

<sup>1</sup>Dipartimento di Scienze della Terra, Università di Siena, Italy, luigidinicola@gmail.com

<sup>2</sup>Institute of Isotope Geochemistry and Mineral Resources, ETH Zurich, Switzerland; strasky@erdw.ethz.ch, wieler@erdw.ethz.ch

<sup>3</sup>Institute of Geological Sciences, University of Bern, Switzerland; akcar@geo.unibe.ch, schluechter@geo.unibe.ch

<sup>4</sup>Dipartimento di Scienze della Terra, Università La Sapienza, Roma, Italy; mariacristina.salvatore@uniroma1.it

<sup>5</sup>Paul Scherrer-Institute, c/o Institute of Particle Physics, ETH Zurich, Switzerland; kubik@phys.ethz.ch

<sup>6</sup>Institute of Particle Physics, ETH Zurich, Switzerland; ivy@phys.ethz.ch

<sup>7</sup>Dipartimento di Scienze della Terra, Università di Pisa, Italy; baroni@dst.unipi.it

**Summary** Glacially scoured morphology characterizes coastal piedmonts in the Terra Nova Bay area. Rounded mountain tops occur below the highest erosional trimlines on the flanks of glacial troughs draining the East Antarctic Ice Sheet (EAIS) and in intervening reliefs. Complex older drifts rest on deglaciated areas above the younger late Pleistocene glacial drift. The authors use geomorphological and glacial geological surveys and surface exposure dating to reconstruct a local chronology of pre-Last Glacial Maximum (LGM) variations of the EAIS and related outlet glaciers. Glacially transported erratics, as well as bedrock surfaces were sampled for cosmogenic-nuclide analysis ( $^{10}\text{Be}$  and  $^{21}\text{Ne}$ ). Bedrock samples show consistent  $^{10}\text{Be}$  and  $^{21}\text{Ne}$  exposure ages indicating exposure since at least 4 Ma with an erosion rate of about 17 cm/Ma; contrary to this, exposure ages of the older drift(s) range from 87 ka to 1352 ka. Furthermore, differences between  $^{21}\text{Ne}$  and  $^{10}\text{Be}$  exposure ages of the erratics indicate complex exposure histories with substantial periods of burial by cold-based ice. Rounded mountain tops represent relict landscape features eroded by the EAIS and its related inter-connected glacier system which overrode the whole coastal area; afterwards, the coastal piedmonts were repeatedly exposed and buried by ice from local and outlet glaciers which did not modify the pre-existing landscape.

**Citation:** Di Nicola L, S. Strasky, C. Schlüchter, M.C. Salvatore, P.W. Kubik, S. Ivy-Ochs, R. Wieler, N. Akçar and C. Baroni (2007), Complex exposure history of pre-LGM glacial drifts in Terra Nova Bay (Victoria Land), using a multiple cosmogenic nuclide approach; in *Antarctica: A Keystone in a Changing World – Online Proceedings of the 10<sup>th</sup> ISAES X*, edited by A.K. Cooper and C.R. Raymond et al., USGS Open-File Report 2007-1047, Extended Abstract 120, 4 p.

### Introduction

Antarctic ice volume regulates global sea level, oceanic and atmospheric circulation and influences the climate on a global scale, with an important part of these interactions governed by the East Antarctic Ice Sheet (EAIS). However, its variations over space and time are not yet fully understood leading to many controversial interpretations (Webb et al. 1984, Webb & Harwood 1991, Denton et al. 1991, Marchant et al. 1993, Schäfer et al. 2000).

In order to shed more light on the dynamics of Antarctic ice masses, it is essential to understand the amplitude and rates of ice volume variations in the past.

These issues are addressed by detailed field mapping and surface exposure dating using the combined application of stable ( $^{21}\text{Ne}$ ) and radioactive ( $^{10}\text{Be}$ ) cosmogenic nuclides.

The aim of the study is the reconstruction of past glacial advances in the Terra Nova Bay area, in northern Victoria Land, a site that is particularly interesting for investigating landscape evolution as it is situated on the margin of the EAIS, and today comprises extensive ice free areas (Fig.1).

### Approach and methods

In order to estimate the timing of glacial advances, erosional surfaces and glacial drifts were identified and selected for the purpose of dating. Detailed geomorphological and glacial geological surveys were carried out on the recent ice-free areas in different sites of the coastal area of Terra Nova Bay, namely the Northern Foothills with the highest summits of Mt. Abbott (1022 m asl) and Mt. Browning (760 m asl). During numerous field traverses, different glacial drifts were distinguished at lower altitudes, and rounded bedrock summits were mapped on



**Figure 1.** Overview map of Terra Nova Bay (Victoria Land); inset shows location of Figure 2.

coastal piedmonts, on glacial valley flanks and on intervening reliefs.

Samples were collected from the mountain tops, below the highest trimline of the area, and from the complex older drifts namely Terra Nova II and Terra Nova III, differentiated by Baroni and Orombelli (1989) and later brought together as older drift by Orombelli et al. (1991). These old deposits rest on the deglaciated areas above the younger late Pleistocene glacial drift Terra Nova I, (Orombelli et al., 1991).

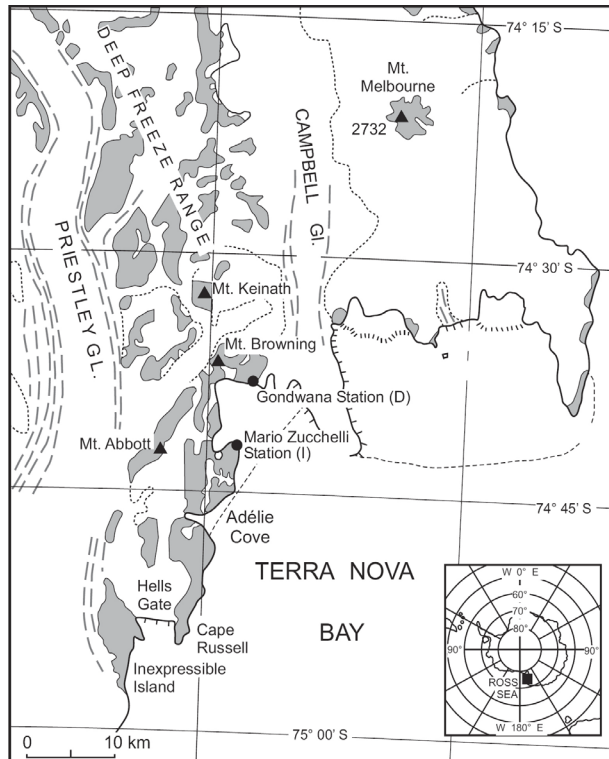


**Figure 2.** Overview map of Northern Foothills (Victoria Land) indicating the sampling sites.

standard models of Lal (1991) and production rates for  $^{10}\text{Be}$  of 5.1 at/g/a (Stone, 2000) and for  $^{21}\text{Ne}$  of 20.33 at/g/a (Niedermann, 2000); all surface exposure ages presented in this work do not include errors for production rates. Scaling of the production rates to altitude and latitude of our sampling sites was conducted after Stone (2000). Corrections were applied for sample thickness and partial shielding from the surrounding topography (Dunne et al., 1999). Details of sampling sites and the minimum exposure ages calculated from measured  $^{21}\text{Ne}$  and  $^{10}\text{Be}$  concentrations are shown in table I.

Because  $^{21}\text{Ne}$  is stable and  $^{10}\text{Be}$  decays in time (half life = 1,5 Ma) the ratio of  $^{21}\text{Ne}/^{10}\text{Be}$  in long-lived samples will increase over time starting from a value  $\sim 4$ , which corresponds to the calculated production rate ratio of  $^{21}\text{Ne}$  and  $^{10}\text{Be}$  at sea level and high latitude.

The two-nuclide plot of Figure 3 is useful for visualizing such ratio changes. The plot has two bounding curves (black lines) derived from analytic solutions for the constant exposure/no-erosion case (lower line) and for the steady-erosion case (upper line).

In the case of continuous exposure and no erosion, the ratio will increase following the lower boundary. In the case of erosion, it will move on a line which is shifted to the left (blue lines). With increasing erosion rate, the line will be shifted to the left. All the lines (for all different erosion rates) in the diagram of Figure 3 will stop at an end point, due to the fact that beryllium will reach saturation when production equals the loss through radioactive decay. By linking all the end-points, we are able to draw a steady-state erosion line. Samples with continuous exposure histories plot within the steady-state erosion line and the no-erosion line. Depending on the erosion rate, they will lie on different lines, but always inside the closed area. Samples plotting above the upper curve are the results of a complex exposure/burial history, with periods of exposure during which the cosmogenic nuclides accumulate, and with intermittent periods of burial (or complete shielding) from cosmic rays during which the radionuclide activity diminishes (and consequently the  $^{21}\text{Ne}/^{10}\text{Be}$  ratio increases).

Bedrock surface from the top of Mt. Abbott (sample ABL1), as well as glacially transported erratics from Mt. Abbott area (samples ABB1-10) and Mt. Browning area (samples BROW1-8) were sampled collecting granites and sandstones in order to be able to use the multi-nuclide approach ( $^{10}\text{Be}$  and  $^{21}\text{Ne}$ ) using quartz as target mineral (see Figure 2 for sampling sites). Samples were chosen where post-depositional overturning of the boulder (in the case of erratics) was unlikely and where field evidence suggested the lowest erosion rates. In the case of evident weathering (pit holes or tafoni affecting the surface), the samples were taken at a spot between the depressions, at a protruding surface which retained surface oxidation and/or rock varnish (confirming no erosion since presence of varnish). Whenever possible, samples were taken from the top of the boulder, or a highly elevated part of bedrock to reduce the probability of shielding by snow, and from the center of the block, where the production rate is reduced due to the escape of neutrons at the edges (Masarik and Wieler, 2003). Sample preparation for neon and for beryllium was done according the standard procedure of Kohl and Nishiizumi (1992), Ivy-Ochs (1996) and Ochs and Ivy-Ochs (1997). Quartz was separated at the laboratory of the University of Bern; beryllium measurements were carried out at the AMS tandem facility at PSI/ETH Zürich and neon analyses were done in the noble gas laboratory of ETH Zurich.

## Results

Single nuclide exposure ages were computed using the

standard models of Lal (1991) and production rates for  $^{10}\text{Be}$  of 5.1 at/g/a (Stone, 2000) and for  $^{21}\text{Ne}$  of 20.33 at/g/a (Niedermann, 2000); all surface exposure ages presented in this work do not include errors for production rates. Scaling of the production rates to altitude and latitude of our sampling sites was conducted after Stone (2000). Corrections were applied for sample thickness and partial shielding from the surrounding topography (Dunne et al., 1999). Details of sampling sites and the minimum exposure ages calculated from measured  $^{21}\text{Ne}$  and  $^{10}\text{Be}$  concentrations are shown in table I.

Because  $^{21}\text{Ne}$  is stable and  $^{10}\text{Be}$  decays in time (half life = 1,5 Ma) the ratio of  $^{21}\text{Ne}/^{10}\text{Be}$  in long-lived samples will increase over time starting from a value  $\sim 4$ , which corresponds to the calculated production rate ratio of  $^{21}\text{Ne}$  and  $^{10}\text{Be}$  at sea level and high latitude.

The two-nuclide plot of Figure 3 is useful for visualizing such ratio changes. The plot has two bounding curves (black lines) derived from analytic solutions for the constant exposure/no-erosion case (lower line) and for the steady-erosion case (upper line).

In the case of continuous exposure and no erosion, the ratio will increase following the lower boundary. In the case of erosion, it will move on a line which is shifted to the left (blue lines). With increasing erosion rate, the line will be shifted to the left. All the lines (for all different erosion rates) in the diagram of Figure 3 will stop at an end point, due to the fact that beryllium will reach saturation when production equals the loss through radioactive decay. By linking all the end-points, we are able to draw a steady-state erosion line. Samples with continuous exposure histories plot within the steady-state erosion line and the no-erosion line. Depending on the erosion rate, they will lie on different lines, but always inside the closed area. Samples plotting above the upper curve are the results of a complex exposure/burial history, with periods of exposure during which the cosmogenic nuclides accumulate, and with intermittent periods of burial (or complete shielding) from cosmic rays during which the radionuclide activity diminishes (and consequently the  $^{21}\text{Ne}/^{10}\text{Be}$  ratio increases).

**Table 1.** Details of sampling sites and the minimum exposure ages calculated from measured  $^{21}\text{Ne}$  and  $^{10}\text{Be}$  concentrations.

	altitude [m asl]	correction factor	$^{21}\text{Ne}$ age [ka]	$^{10}\text{Be}$ age [ka]
ABL-1	1022	0.96	2219 +/- 85	1719 +/- 86
ABB1	596	0.98	349 +/- 44	143 +/- 7
ABB2	596	0.97	217 +/- 29	134 +/- 5
ABB3	608	0.87	222 +/- 31	163 +/- 8
ABB4	519	0.87	311 +/- 23	143 +/- 5
ABB7	500	0.95	1352 +/- 74	533 +/- 27
ABB10	393	0.95	1058 +/- 48	469 +/- 23
BROW1	470	0.94	510 +/- 39	356 +/- 14
BROW2	474	0.97	225 +/- 28	87 +/- 4
BROW3	505	0.96	1085 +/- 52	617 +/- 26
BROW7	674	0.96	251 +/- 20	133 +/- 7
BROW8	661	0.96	140 +/- 15	125 +/- 6

Figure 3 shows all our new data in this two-nuclide diagram. If we consider the results obtained from the erratic boulders collected in the coastal area, the cosmogenic  $^{21}\text{Ne}$  concentrations are in excess of that expected from the radioactive  $^{10}\text{Be}$  activity. The  $^{21}\text{Ne}/^{10}\text{Be}$  ratios are significantly higher than expected for continuous exposure, implying a complex exposure history. On the other hand, the sample collected from bedrock at the top of Mt. Abbott (ABL-1) plots inside the closed area indicating continuous exposure and an erosion rate of  $17\pm 2$  cm/Ma.

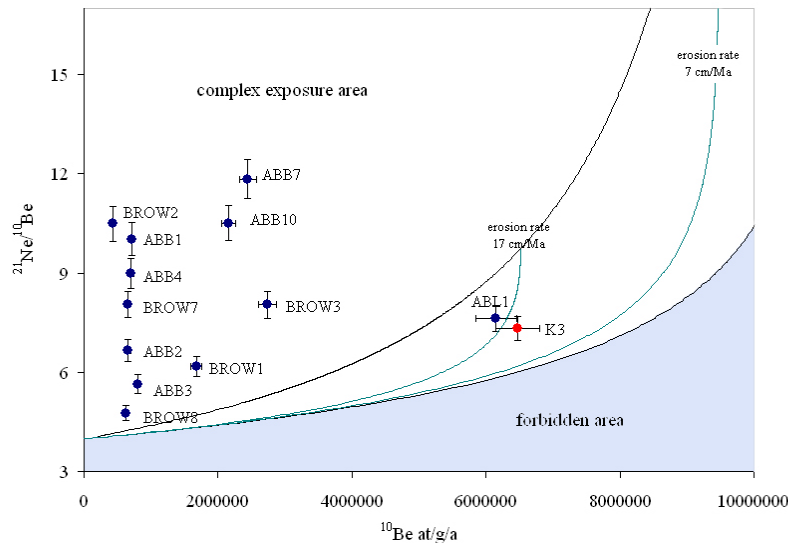


**Figure 3.** Two nuclides plot indicating complex exposure history for all the erratic boulders and continuous exposure history and erosion rate of 17 cm/Ma for ABL-1; in red, bedrock sample K3 from Mt. Keinath (Oberholzer et al., 2003).

## Discussion

These cosmogenic exposure ages suggest two different glacial histories for the summit area and the erratic boulders from lower elevations. The samples plotting in the “complex exposure history” area suggest an exposure period interrupted by one or more episodes of burial (or total shielding) by almost non-eroding ice. A different history is shown for the top of the mountains, where an old glacially eroded landscape is preserved. The  $^{21}\text{Ne}/^{10}\text{Be}$  ratio of ABL-1 suggests that this sample has experienced a continuous history of exposure without burial or temporal shielding (e.g. by seasonal snow-cover). The resulting two-nuclide erosion rate is  $17\pm 2$  cm/Ma. Considering this erosion rate, the neon exposure age shifts from  $2.2\pm 0.1$  to  $3.8\pm 0.1$  Ma and the beryllium exposure age from  $1.9\pm 0.1$  to  $3.7\pm 0.1$  Ma. This result is in agreement with the findings of Oberholzer et al. (2003) for the age of the top of Mt. Keinath (1090 m asl), in the northern part of the Northern Foothills. Recalculating the exposure data with sea level high latitude production rates of 5.1 at/g/a for  $^{10}\text{Be}$  and 20.33 at/g/a for  $^{21}\text{Ne}$ , results in an erosion rate of  $16\pm 2$  cm/Ma and shifts the  $^{21}\text{Ne}$  age from  $2.3\pm 0.1$  to  $3.6\pm 0.1$  Ma and the  $^{10}\text{Be}$  age from  $1.9\pm 0.1$  Ma to  $3.6\pm 0.1$  Ma.

## Implications

$^{10}\text{Be}$  and  $^{21}\text{Ne}$  surface exposure ages obtained from glacially scoured bedrock on the summit of Mt. Abbott show that the mountains in the Northern Foothills, have been free of ice for at least 4 Ma. This implies that the Transantarctic

Mountains have not been overridden by erosive ice after the mid-Pliocene. Since then, erosion has been very low, with denudation rates of 16 to 17 cm/Ma, allowing the preservation of relict surfaces. The erratic boulders preserved in the lower areas were repeatedly exposed and buried by low-erosive ice from local and/or outlet glaciers, which did not modify the pre-existing landscape.

## Conclusions

This study presents one of the first combined applications of noble gas and radionuclide analyses. Although the data discussed here do not allow for the creation of a detailed glacial chronology, however some relevant constraints for the sample histories can be obtained. The exposure data obtained from bedrock suggest the preservation of the mountain tops of Terra Nova Bay area over millions of years. There is evidence that the summit areas of Mt. Abbott and Mt. Keinath were sculpted by wet-based ice before at least 4 Ma and that they have not been glacially modified since. The excess of cosmogenic neon over cosmogenic beryllium measured in the erratic boulders is interpreted as result of periods of burial by non-erosive ice suggesting a cold and hyperarid climate. These findings show the importance of combined stable and radioactive cosmogenic isotopes for the interpretation of exposure data of glacial drifts in Antarctica. Only with a multiple nuclide approach, is it possible to detect a complex exposure history such as burial of a surface by ice, which does not modify the pre-existing landscape.

## Summary

Surface exposure dating and detailed field geomorphologic and glacial geological surveys were applied to construct the glacial history of Terra Nova Bay area. The results show that the summit areas of the Northern Foothills were sculpted at least 4 Ma ago by wet-based ice and that they have not been glacially modified since. The complex glacial drifts at lower elevation had experienced periods of burial by non-erosive ice suggesting a cold and hyperarid climate.

**Acknowledgements:** This work was carried out through a joint research program of the School of Polar Science of Siena, Department of Earth Science of Pisa, and the Institutes of Geological Science of Bern and ETH of Zurich. It was supported by the Italian National Program on Antarctic Research (PNRA) and the Swiss National Science Foundation (grant. No. 200020-105220/1). The support by all Italian and Swiss colleagues of the XX and XXI Expeditions is gratefully acknowledged.

## References

- Baroni, C. (1989), Geomorphological map of the Northern Foothills near the Italian Station, (Terra Nova Bay, Antarctica). *Memorie della Società Geologica Italiana*, 33 (1987), 195-211.
- Baroni, C., and G. Orombelli (1989), Glacial geology and geomorphology of Terra Nova Bay (Victoria Land, Antarctica), *Memorie della Società Geologica Italiana*, 33 (1987), 171-193.
- Baroni, C. (Ed.), A. Biasini, A. Bondesan, G.H. Denton, M. Frezzotti, P. Grigioni, M. Meneghel, G. Orombelli, M. C. Salvatore, A. M. Della Vedova and L. Vittuari (2005) - Mount Melbourne Quadrangle, Victoria Land, Antarctica 1:250,000 (Antarctic Geomorphological and Glaciological Map Series). In: Haerberli W., Zemp M., Hoelzle M. & Frauenfelder R. (eds.), 2005, *Fluctuations of Glaciers. A contribution to the Global Environment Monitoring Service (GEMS) and the International Hydrological Programme, Vol VIII (1995-2000)*, pp. 38-40. World Glacier Monitoring Service, International Association of Hydrological Sciences (International Commission on Snow and Ice), United Nations Environment Programme, and United Nations Educational, Scientific and Cultural Organization, Zürich.
- Denton, G. H., M. L. Prentice, and L. H. Burckle (1991), Cenozoic history of the Antarctic ice sheet. In TINGEY, R.J., ed. *The geology of Antarctica*. Oxford, England:Oxford University Press, 365-433.
- Dunne, J., D. Elmore, and P. Muzikar (1999), Scaling factors for the rates of production of cosmogenic nuclides for geometric shielding and attenuation at depth on sloped surfaces, *Geomorphology*, 27, 3-11.
- Ivy-Ochs, S. (1996). The dating of rock surfaces using in situ produced Be-10, Al-26 and Cl-36, with examples from Antarctica and the Swiss Alps. PhD thesis, ETH Zürich.
- Kohl, C. P., and K. Nishiizumi (1992), Chemical isolation of quartz for measurement of in-situ-produced cosmogenic nuclides, *Geochimica Cosmochimica Acta*, 56, 3583-3587.
- Lal, D. (1991), Cosmic ray labelling of erosion surfaces: in situ nuclide production rates and erosion models, *Earth Planetary Science Letters*, 104, 424-439;
- Marchant, D.R., G.H. Denton., D.E. Sugden, and C.C. Swisher (1993), Miocene glacial stratigraphy and landscape evolution of the Western Asgard Range, Antarctica. *Geografiska Annaler*, 75A, 303-330.
- Masarik, J. and R. Wieler (2003), Production rates of cosmogenic nuclides in boulders. *Earth and Planetary Science Letters*, 216:201-208.
- Niedermann, S. (2000), The <sup>21</sup>Ne production rate in quartz revisited, *Earth and Planetary Science Letters*, 183, 361-364.
- Oberholzer, P., C. Baroni, J. Schaefer, G. Orombelli, S. Ivy-Ochs, P.W. Kubik, H. Baur, R. Weiler (2003), Limited Pliocene/Pleistocene glaciation in Deep Freeze Range, northern Victoria Land, Antarctica, derived from in situ cosmogenic nuclides, *Antarctic Science* 15, (4), 493-502;
- Ochs, M., and S. Ivy-Ochs (1997), The chemical behavior of Be, Al, Fe, Ca and Mg during AMS target preparation from terrestrial silicates modeled with chemical speciation calculations, *Nuclear Instruments and Methods in Physics Research B*, 123, 235-240.
- Orombelli G., C. Baroni, G.H. Denton (1991), Late Cenozoic glacial history of the Terra Nova Bay region, northern Victoria Land, Antarctica, *Geografia Fisica e Dinamica Quaternaria*, 13 (2, 1990), 139-163.
- Schäfer, J., H. Baur, G.H., Denton, S. Ivy-Ochs, D.R. Marchant, C. Schlüchter., and R. Wieler (2000), The oldest ice on earth in Beacon Valley, Antarctica: New evidence from surface exposure dating. *Earth and Planetary Science Letters*, 179,91-99.
- Stone, J. O. (2000), Air pressure and cosmogenic isotope production, *Journal of Geophysical Research B*, 105, 23753-23759.
- Webb, P.N. and D.M. Harwood (1991), Late Cenozoic glacial history of the Ross Embayment, Antarctica. *Quaternary Science Reviews*, 10, 215-223.
- Webb, P.N., D.M. Harwood, B.C. Mckelvey, J.H. Mercer, and L.D. Stott (1984). Cenozoic marine sedimentation and ice volume variation on the East Antarctic craton. *Geology*, 12, 287-291.